

Original papers

Near infrared computer vision and neuro-fuzzy model-based feeding decision system for fish in aquaculture



Chao Zhou^{a,b,c,d}, Kai Lin^{a,b,c}, Daming Xu^{a,b,c}, Lan Chen^{a,b,c}, Qiang Guo^{a,b,c}, Chuanheng Sun^{a,b,c,*}, Xinting Yang^{a,b,c,*}

^a Beijing Research Center for Information Technology in Agriculture, Beijing 100097, China

^b National Engineering Research Center for Information Technology in Agriculture, Beijing 100097, China

^c National Engineering Laboratory for Agri-product Quality Traceability, Beijing 100097, China

^d School of Automation, Beijing Institute of Technology, Beijing 100081, China

ARTICLE INFO

Keywords:

Aquaculture

Feeding behavior

Feeding optimization

Image processing

Adaptive network-based fuzzy inference system

ABSTRACT

In aquaculture, the feeding efficiency of fish is of great significance for improving production and reducing costs. In recent years, automatic adjustments of the feeding amount based on the needs of the fish have become a developing trend. The purpose of this study was to achieve automatic feeding decision making based on the appetite of fish. In this study, a feeding control method based on near infrared computer vision and neuro-fuzzy model was proposed. The specific objectives of this study were as follows: (1) to develop an algorithm to extract an index that can describe and quantify the feeding behavior of fish in near infrared images, (2) to design an algorithm to realize feeding decision (continue or stop) during the feeding process, and (3) to evaluate the performance of the method. The specific implementation process of this study was as follows: (1) the quantitative index of feeding behavior (flocking level and snatching strength) was extracted by Delaunay Triangulation and image texture; (2) the adaptive network-based fuzzy inference system (ANFIS) was established based on fuzzy control rules and used to achieve automatically on-demand feeding; and (3) the performance of the method was evaluated by the specific growth rate, weight gain rate, feed conversion rate and water quality parameters. The results indicated that the feeding decision accuracy of the ANFIS model was 98%. In addition, compared with the feeding table, although this method did not present significant differences in promoting fish growth, the feed conversion rate (FCR) can be reduced by 10.77% and water pollution can also be reduced. This system provides an important contribution to realizing the real-time control of fish feeding processes and feeding decision on demand, and it lays a theoretical foundation for developing fine feeding equipment and guiding practice.

1. Introduction

Currently, the development of intensive aquaculture has led to increases in the proportion of feed among the total costs, and these values in certain species can reach 86% (Rola and Hasan, 2007). Therefore, determining when to start or stop feeding during the production process is important. Unreasonable feeding leads to economic losses, and the uneaten feed and fish feces also pollute the environment. These factors should be considered when developing accurate tools for managing production and feeding (Wu et al., 2015; Zhou et al., 2017a).

Additional problems are associated with feeding fish compared with feeding livestock. To date, artificial feeding control methods are widely used in production. Although predicting when feeding should be stopped may be intuitive, this information is often influenced by the

subjective experience of the observer and cannot be quantified by a unified standard (Mallekh et al., 2003). In recent years, the increased understanding of fish behavior and the continuous development of new technologies have led to new feeding technologies. However, numerous factors affect fish intake, including physiological, nutritional, environmental and management factors (Sun et al., 2016). All of the above factors can be expressed via fish behavior. For example, the feeding frequency and time will lead to different feeding intensity of fish, the direction of movement of fish can vary depending on how the feed was sprinkled. Studies have demonstrated that the speed or direction of the movement of fish during feeding can be used to determine the appetite of fish (Martins et al., 2012; Pinkiewicz et al., 2011). These behavioral data are critical to the development of intelligent management strategies or systems (Sun et al., 2016; Xu et al., 2006; Zion, 2012). According

* Corresponding authors at: Shuguang Huayuan Middle Road 9#, Haidian District, Beijing 100097, China.

E-mail address: yangxt@nercita.org.cn (X. Yang).

to the latest review by Zhou et al. (2017a), the amount of feeding may be automatically adjusted according to the actual needs of fish based on the appetite of fish, and this topic has become a trend of research and development.

Numerous scholars have developed feeding methods or systems that can realize the real-time calculation of feed demand based on the quantity of fish. Feeding systems are equipped with a variety of monitoring and feedback devices that can automatically determine the feeding demands of fish. Machine vision, underwater acoustic technology, and water quality sensors are commonly used to obtain information regarding feeding behavior and its attributes. For instance, fish appetite was evaluated by detecting and counting pellets via computer vision, and then the feeds were automatically supplied (Li et al., 2017). Simultaneously, acoustic sensors can be used to detect feed and may act as an indicator to judge the appetite of fish (Juell et al., 1993). This system can avoid feed waste and promote fish growth. Changes in water quality parameters can also affect the appetite of fish. Temperature and dissolved oxygen are the two most important parameters. This information can be used as the input to an intelligent control model or algorithm to provide precise food quantities (Soto-Zarazúa et al., 2010). The biomass of cultured fish is directly related to the feeding amount and has been used to predict the daily feed demand of fish (Loo, 2013; Papandroulakis et al., 2000). In addition, an intelligent feedback control system based on infrared photoelectric sensors can be used to obtain fish aggregation behavior. Combined with a specific control algorithm, the feeding machine can automatically stop feeding based on the aggregation behavior observed during the process of feeding fish (Chang et al., 2005).

All of these methods have advantages, disadvantages, and most suitable applications. The acoustic method is suitable for use in a large-volume aquaculture model. However, the cost of the method is high, and developing is difficult. Among these methods, computer vision technology has been widely used to analyze and quantify the behavior parameters in the feeding process because of its low cost and lack of damage to fish (Lin et al., 2018). For example, the scatter and movement intensity of populations related to the appetite of rainbow trout (Sadoul et al., 2014), salmon (Liu et al., 2014), tilapia (Zhangying et al., 2016; Zhao et al., 2017, 2016) and sole (Duarte et al., 2009) were studied using computer vision. Various feeding behavior quantification indexes, such as the image processing activity index (IPAI) (Duarte et al., 2009) and computer vision-based feeding activity index (CVFAI) (Liu et al., 2014), were extracted. However, traditional computer vision requires better illumination conditions when collecting images. In most fish farms, light is typically insufficient and uneven; therefore, near infrared computer vision may be useful. Near infrared machine vision, which is based on traditional machine vision, offers most advantages of traditional computer vision, and most of the associated image processing algorithms are common to conventional computer vision methods (Zhou et al., 2017a). Combined with certain image enhancement algorithms, this methodology can also achieve better imaging results under poor illumination conditions (Farokhi et al., 2016; Hung et al., 2016; Zhou et al., 2017b). Moreover, this system does not affect normal growth and does not cause stress on fish (Shcherbakov et al., 2013). Therefore, this system is suitable for aquaculture farms where light is insufficient, especially in a recirculating aquaculture system (RAS). In fact, near infrared computer vision systems were previously used for fish behavior monitoring, and the 3D position of fish was estimated by calculating the brightness of fish in the near infrared image (Pautsina et al., 2015). Zhou et al. (2017c) performed a similar study. The behavior of fish during feeding was monitored, and the flocking index was extracted. Thus, the process of feeding behavior was well described, and the feasibility of near infrared computer vision for behavior analysis and intelligent feeding control was demonstrated.

However, all of the above approaches exhibit a common problem in making precise feeding decisions. Thus, after quantifying the behavior or growth status, most previous studies only considered one feeding

behavior index when selecting the threshold to continue or stop feeding and did not combine or directly ignored other behavior quantitative indexes. In general, the feeding behavior of fish is manifested in several forms, and using a single index will likely cause errors. Furthermore, the selection process is typically realized via many tests, a lack of self-learning ability and low intelligence; thus, it does not provide a true sense of intelligent feeding control. With the development of intelligent optimization algorithms, it is possible to apply adaptive algorithms to feeding control processes. The adaptive network-based fuzzy inference system (ANFIS) integrates the concept of fuzzy logic into neural networks and has been widely used in numerous engineering science and aquaculture system applications (Jang, 1993). Previous studies have demonstrated the feasibility of using ANFIS for feeding control (Wu et al., 2015). The principle was that when the fish searches for food, its activity leads to changes in the concentration of dissolved oxygen, which can be used to quantify the feeding behavior. Then, the feeding behavior quantification index was used as the input of ANFIS to realize feeding control. Furthermore, ANFIS was also used to assess water quality (Carbajal-Hernández et al., 2012), optimize fishing predictions (Iglesias Nuno et al., 2005).

Based on the simulation of a commercial-scale fish farm, the current study proposes a feeding decision method in aquaculture. Near infrared computer vision was used to quantify the feeding behavior, and then the quantified index factors were used as the input of the ANFIS model. The overall goal of this study was to achieve automatic feeding control according to the appetite of fish, thereby improving the applicability of feeding control methods in aquaculture. The specific objectives included: (1) developing an algorithm to extract an index that can describe and quantify the feeding behavior of fish in near infrared images, (2) designing an algorithm to realize the intelligent control to continue or stop the feeding process, and (3) evaluating the performance of the method.

2. Materials and methods

Feeding involves complex system engineering. Here, the studied method cannot solve all feeding problems and exhibits a most suitable application occasion or breeding species. This system was applicable to swimming fish species, such as carp, salmon, and tilapia. Fixed-point feeding was recommended. A schematic of the system is presented in Fig. 1.

2.1. Experimental materials

Tilapia was selected for this study. All tilapia were provided by the Xiao Tangshan Aquaculture Breeding Development Center (Changping, Beijing, China). Before used in the experiment, the fish were raised for four weeks to adapt to the experimental culture environment. During acclimation, the fish (30 tilapias with 138 ± 4 g in each tank) were fed floating pellets (Youyi Hongyuan Co. Ltd., Beijing, China) twice a day (8:00 and 16:00). During each feeding, fixed-point feeding was used to deliver the pellet feed to fish. The feeding rate was set to 2% per day. The oxygen level was maintained within the range of 5.8–8.2 mg/L, and water temperature was maintained at 20–25 °C.

2.2. Experimental system

The experiment was performed in the RAS laboratory of the Xiaotangshan National Experiment Station for Precision Agriculture (Changping, Beijing, China). A previously described experimental setup was used (Fig. 2) (Zhou et al., 2018, 2017b,c). The system consists of 6 tanks (diameter of 1.5 m and water depth of 1 m). Image acquisition and processing were achieved using an industrial camera (Mako G-223B, Advanced Vision Technology (AVT), Stadroda, Germany), an 8-W light source (MVIR0460, HEROWEI, Guangdong, China) and a computer (Intel® Core™ i5-4590 CPU@3.30 GHz, 4.00 GB RAM). The

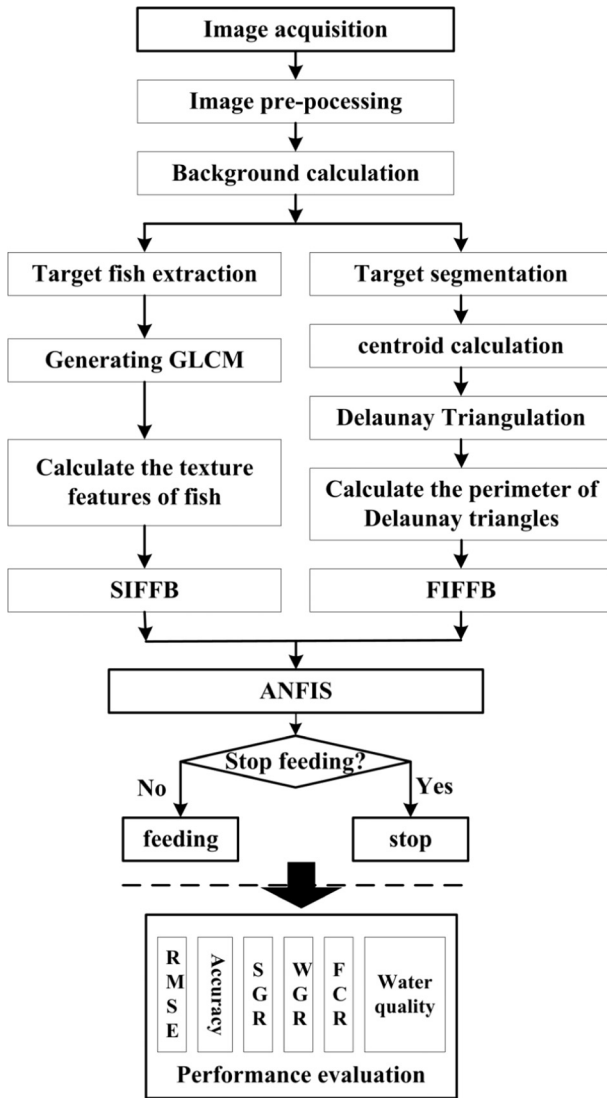


Fig. 1. Schematic of the method.

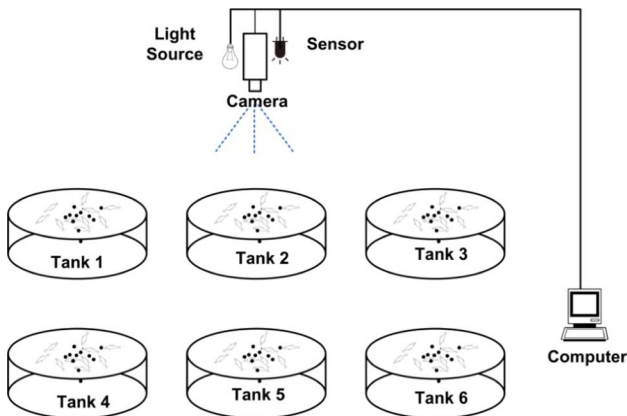


Fig. 2. Experimental system.

image of tank was captured one by one. The raw output data stream from the camera was converted to BMP files via software we developed using software packages provided by AVT. To reduce errors caused by water surface fluctuations, bubbles, and foam on the image processing results, the water inlet was submerged below the water surface, and the water flow entered the tank in a tangential direction.

2.3. Image processing and feeding behavior index extraction

The image processing methods used in this paper were based on studies by Pautsina et al. (2015) and Zhou et al. (2017c). The average background method and background subtraction were used to obtain the background (Downey and Koutsopoulos, 1993). After background subtraction and image contrast enhancement (Zhou et al., 2017b), the quantitative index of feeding behavior was extracted using Delaunay Triangulation (DT) and image texture.

2.3.1. Flocking index of fish feeding behavior

After enhancement, the image was segmented and the feature was extracted to obtain the targets of the image. The target was filtered according to the size of the fish, and targets that were too large or too small were removed to obtain the binary image of the fish. The centroid of the fish was calculated using order moments (Moreda et al., 2012) to characterize the fish position (Fig. 3a). Then, the centroid was used as the vertex point of the Delaunay triangle. After DT, Delaunay triangles were obtained (Fig. 3b).

In the Delaunay triangle, the three vertices of each triangle corresponded to the smallest circumscribed circle. Thus, the size of each triangle reflected the distance between the vertices. For each image, the average perimeter of the triangle in the Delaunay triangulation network reflected the flocking level of fish stocks. Therefore, the flocking index of fish feeding behavior (FIFFB) can be expressed as Eq. (1):

$$\text{FIFFB} = \frac{\sum_{i=1}^n P_i}{n} = \frac{\sum_{i=1}^n (L_{i1} + L_{i2} + L_{i3})}{n} \quad (1)$$

where n represents the number of Delaunay triangles. For the i -th triangle, P_i is the circumference and L_{i1} , L_{i2} and L_{i3} are the lengths of three edges. The FIFFB is the average perimeter of all triangles in Delaunay Triangulation, and it represents the flocking level of fish. A lower FIFFB value indicates an increased flocking level.

2.3.2. Snatch intensity of fish feeding behavior

Image texture analysis is an important field of computer vision research. At any given time and space, the surface of any object will exhibit a texture. Moreover, the texture feature of the image is independent of the color information of the image, and this information can reflect the spatial composition characteristics of different images. Therefore, the intensity of feeding activity of fish populations can be analyzed using this feature of texture. When analyzing the texture features, the feature parameters that describe image texture information can be extracted based on the gray level co-occurrence matrix (GLCM). These data can reflect gray information regarding the direction, the adjacent interval and the range of change. This system serves as the basis for analyzing local patterns and pixel arrangement rules. GLCM parameters can accurately represent the texture information of the image, including contrast, energy, correlation, and homogeneity (Hu et al., 2012; Mollazade et al., 2013).

In this paper, the contrast was used to characterize the strength of snatch fish. The contrast reflects the clarity and the depth of the image texture groove. A deeper texture of the groove indicates increased contrast, and the visual effect will be clearer. When fish exhibit violent snatching, the texture of the groove is deeper, and the contrast is greater. Therefore, the contrast of the texture intensity information can be used to describe the fish feeding process. The snatch intensity of fish feeding behavior (SIFFB) can be defined as Eq. (2):

$$\text{SIFFB} = \sum_{i=1}^N \sum_{j=1}^N (i-j)^2 P(i,j,d,\theta) \quad (2)$$

where $P(i, j, d, \theta)$ is the GLCM; N is the image gray scale series; i and j are the gray values of the image; d is the step of 2 pixels; and θ is the angle between the two points. In this study, after the images of the fish feeding process were collected, the background images were obtained

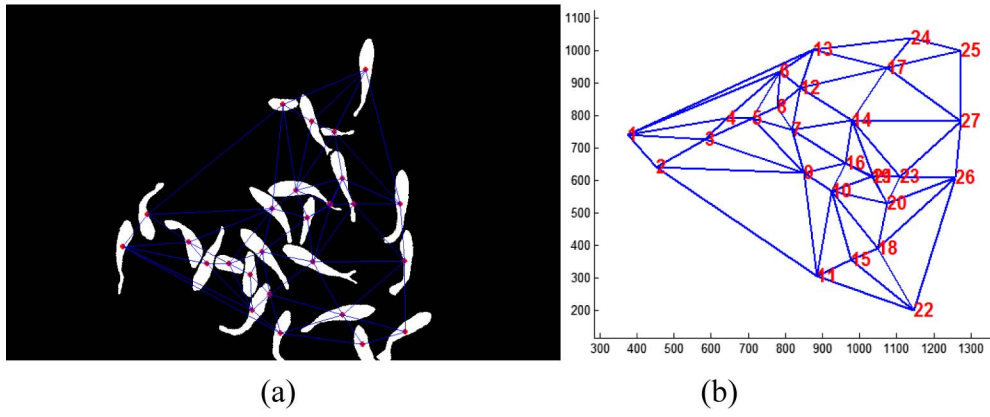


Fig. 3. Delaunay Triangulation. (a) Centroid of fish; and (b) results of Delaunay Triangulation.

via the mean background method. Then, the foreground target fish was extracted by background subtraction, and the GLCM was generated. Finally, the SIFFB was obtained.

2.4. Adaptive network-based fuzzy inference system

The ANFIS model was proposed by Jang (1993). This model is both an inheritance and an extension of the traditional fuzzy reasoning system. The fuzzy modeling can make full use of expert knowledge and reasoning capabilities without the need for accurate quantitative analysis. But the disadvantage is that there is no common learning method to transfer the experts' knowledge and experience into the rule base and fuzzy inference system. There is also no effective way to adjust the fuzzy membership function to minimize the output error or maximize the performance. Compared with the traditional fuzzy reasoning system, the ANFIS model not only extracts linguistic rules from the expertise of experts, but also optimizes models using input and output data. By adjusting the membership function, the model fits well with the given data. Therefore, ANFIS has prominent advantages for the modeling of nonlinear objects. In the ANFIS model, the neural networks provide a learning mechanism to make a decision, select fuzzification component models, and assess the uncertainties or inaccuracies of the behavior and decision parameters. This model combines a fuzzy inference system with a neural network to offer self-organizing learning (Sefeedpari et al., 2014).

The ANFIS model consists of two parts: a rule base and a database. The rule base contains a series of fuzzy “if-then” rules, and the database defines the membership functions (MF) of the fuzzy sets in the fuzzy rules. The two components constitute the knowledge base of the inference system. The reasonable membership function can be adjusted gradually using the established rule base. Thus, the fuzzy reasoning system is more consistent with the actual input and output situation. The input variables of the fuzzy reasoning system were fuzzified first, and then the fuzzy output variables were obtained from the decision logic unit. Finally, the final output was obtained by the de-fuzzification module (Virgen-Navarro et al., 2016).

For simplicity, consider a fuzzy reasoning system with two inputs x , y and an output f . For a first-order fuzzy model inference system of the Sugeno type consisting of n rules, if the i -th rule is defined as Rule i , then,

$$\text{Rule } i: \text{ if } x \text{ is } A_i \text{ and } y \text{ is } B_i, \text{ then } f_i = p_i x + q_i y + r_i \quad (3)$$

where x and y are input variables and A_i and B_i are linguistic variables. Here, p_i , q_i , and r_i in the i -th rule were determined by the measured data, and these values reflect the inherent characteristics of the system. As shown in Fig. 4, the set of “if-then” rules represents the reasoning mechanism of the Sugeno fuzzy model, whereas w_i represents the firing strength of the i -th rule. This model has two components as specified: a

premise and consequent part.

In the Sugeno fuzzy model, the parameters of the model output function are unknown. To implement the fuzzy logic controller (FLC) model, these parameters must be determined by ANFIS, and the structure is presented in Fig. 5. This method can realize the mapping process from the given input to the output using fuzzy logic to achieve feeding decision-making control. In Fig. 5, the same layer of network nodes has the same function type. The model consists of 5 layers, in which each output signal from the upper layer is the input to the nodes of the next layer (Jang, 1993). A detailed introduction of the system is provided.

Layer 1: Input layer. All nodes are adaptive nodes. The input variables are mapped to the fuzzy set, and the membership was calculated. In this study, the bell-shaped membership function was used, which was performed as follows:

$$O_i^1 = \mu_{A_i}(x) = \frac{1}{1 + \left| \frac{x - a_i}{a_i} \right|^{2b_i}} \quad (4)$$

where O_i^j represents the i -th node of layer 1, x is the input to node i , and A_i is the linguistic label (big, small, etc.) associated with this node function. Here, $\{a_i, b_i, c_i\}$ are the parameters that change the shape of the membership function, which is called the premise parameter.

Layer 2: Rule layer. All nodes of this layer are fixed nodes. The precondition of fuzzy rules between variables was matched and the weight value of each rule was obtained, that is, the firing strength w_i calculated as follows:

$$O_i^2 = w_i = \mu_{A_i}(x) \cdot \mu_{B_i} \quad (5)$$

Layer 3: Weighted average. Every node in this layer is a circle node labeled N . The i -th node calculates the ratio of the i -th rule's firing strength to the sum of all rules' firing strengths:

$$O_i^3 = \bar{w}_i = \frac{w_i}{w_1 + w_2 + w_3} \quad (6)$$

For simplicity, the output of this layer was called the normalized firing strength.

Layer 4: Conclusion inference layer. The layer node calculates the contribution of the rule to the final output, and the node function is as follows:

$$O_i^4 = \bar{w}_i f_i = \bar{w}_i (p_i x + q_i y + r_i) \quad (7)$$

where $\{p_i, q_i, r_i\}$ are the consequent parameters of the fuzzy inference.

Layer 5: Output layer. Computes the overall output as the summation of all incoming signals, the node function is as follows:

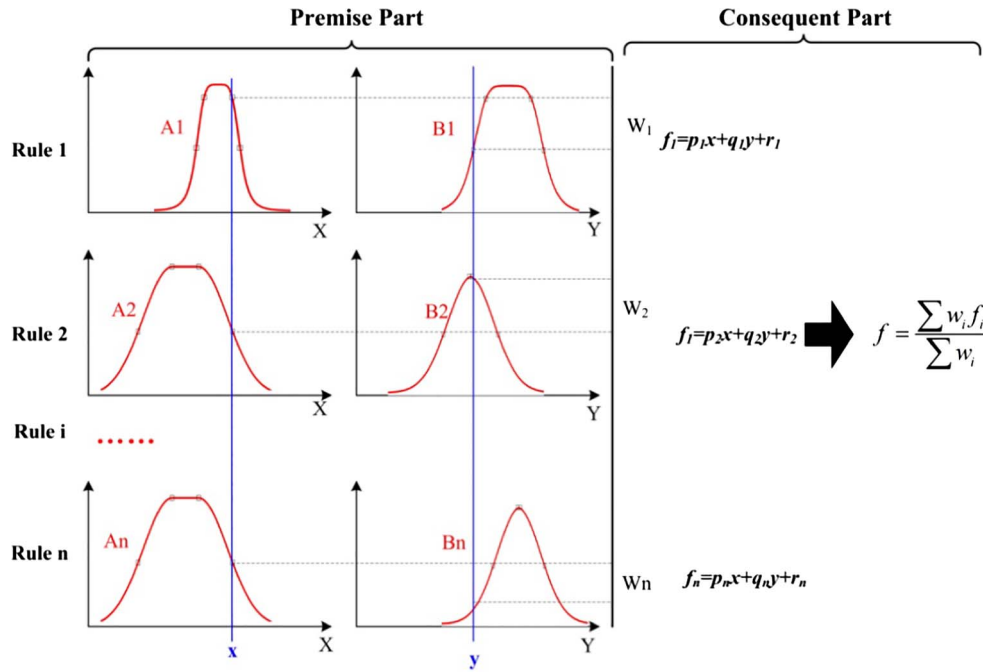


Fig. 4. ANFIS architecture of the constructed fuzzy model.

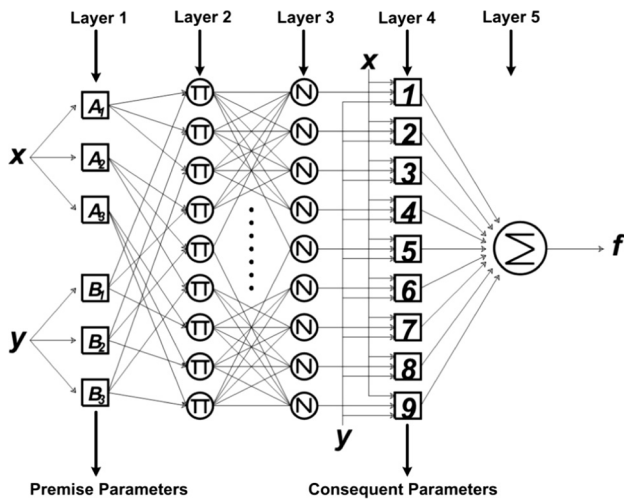


Fig. 5. Two-input first-order Sugeno fuzzy model with 9 rules (Jang, 1993).

$$O_i^5 = \sum_i w_i f_i = \frac{\sum_i w_i f_i}{\sum_i w_i} \quad (8)$$

Through hybrid learning, ANFIS can simulate, model and analyze the mapping relationship between input and output data. Thus, the optimal distribution of membership function can be determined. ANFIS uses gradient descent and least squares to adjust the internal parameters and exhibits high convergence speed. Each step of the hybrid learning algorithm was divided into a forward pass and backward pass, during which signal transfer and parameter adjustment are completed. In the forward pass, the input data and the function signal are transmitted forward. When the signal is transmitted to the fourth layer, the least square method was used to adjust the consequent parameters. In the backward pass, the error signal is transmitted reversely from the system output node to the input node, and the gradient descent method is adopted to adjust the premise parameters (Jang, 1993).

In this paper, the input feeding behavior parameters (FIFB and SIFFB) and the output feeding decision (continue or stop feeding) were

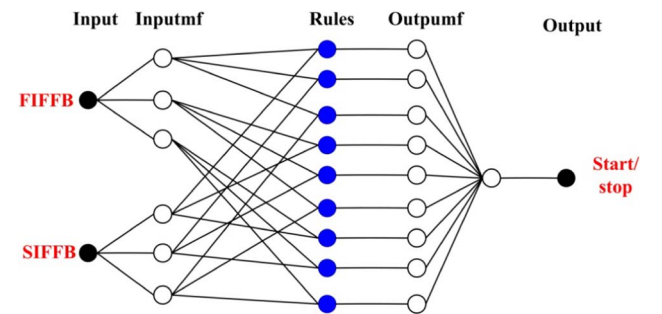


Fig. 6. Architecture of ANFIS.

evaluated in the ANFIS model. A neuro-fuzzy model with the input parameters FIFB and SIFFB and an output of feeding decision was developed to control the decision to continue or stop feeding. The system structure of the model is presented in Fig. 6.

2.5. Method performance evaluation

The ANFIS model performance was validated using the feeding decision accuracy and the root mean square error (RMSE) (Eqs. (9) and (10)). Where $n_{correct}$ is the number of the correct decision, x_i denotes the observed value, \hat{x}_i is the predicted value and n is the number of samples. A lower RMSE indicated better model performance.

$$Accuracy = \frac{n_{correct}}{n} \times 100\% \quad (9)$$

$$RMSE = \sqrt{\frac{1}{n} \sum_{i=1}^n (x_i - \hat{x}_i)^2} \quad (10)$$

The long-term performance of the method was assessed using the fish-specific growth rate (SGR), weight gain rate (WGR) and feed conversion rate (FCR). These parameters are defined in Eqs. (11)–(13). Among them, W_t and W_0 are the average weight of time t and F is the total amount of feed intake.

$$SGR = \frac{\ln W_t - \ln W_0}{t} \times 100\% \quad (11)$$

$$FCR = \frac{F}{W_t - W_0} \quad (12)$$

$$WGR = \frac{W_t - W_0}{W_0} \times 100\% \quad (13)$$

Moreover, to evaluate the impact of the method on water pollution, its performance was evaluated by the turbidity, ammonia nitrogen and pH values. The water quality parameters were obtained through a multi-parameter water quality sensor (Km-Mu, KING MILL Co. Ltd, Shanghai, China). This information can be collected in real time online and supports the water quality data assessment. These data can be saved and exported through a wireless module. The data sampling interval of the sensor was set to 2 s.

3. Results and discussion

3.1. FIFFB and SIFFB

In this experiment, the images during the feeding process were analyzed, and the FIFFB and SIFFB of each frame were extracted and calculated. The curves of the FIFFB and SIFFB during the feeding process are presented in Fig. 7. The red solid line and blue dotted line represent the variation trends of the FIFFB and SIFFB, respectively. As noted in Fig. 7, the SIFFB varies minimally from the 1–26th second, which corresponds to the stage before the fish feeding. In the 28–82nd seconds, and a dramatic fluctuation in the SIFFB was noted, which coincides with the feeding stage of the fish population. After a brief feeding peak, the increase in the FIFFB and the decrease in the SIFFB indicate a reduction in feeding intensity because fish consume large amounts of dissolved oxygen and produce considerable amounts of metabolic waste during feeding (Johansson et al., 2006). However, after the 84th second, the SIFFB gradually returns to the previous state and fish feeding is gradually completed. These data indicate that after a period of snatching, the appetite of fish wanes (Liu et al., 2014). From the 144–150th second, a relatively significant alteration in the SIFFB of partial frames was noted. From the observation of the original image, it was found that individual fish swim to the surface to catch the remaining bait, which is consistent with the feeding situation of fish stocks. The FIFFB and SIFFB exhibit an opposite change relationship. Generally, hunger stimulates feeding behavior in fish. A previous study also demonstrated that when feed was offered, fish may initially feed at a faster rate and slowly decrease or stop with a gradual reduction in appetite (Lall and Tibbetts, 2009). Fig. 8 are examples images of individual stages. Thus, a phenomenon was noted that when the fish snatched food violently, the FIFFB decreased, whereas the SIFFB increased, and vice versa. Therefore, these two parameters can better describe the feeding process that can be used as the input of the ANFIS model.

3.2. Results and performance of the ANFIS model

In this paper, the input value and the output of the fuzzy controller were realized to obtain the intelligent feeding control. The parameters of the ANFIS model were set as follows: step size, 0.01; step size decrease rate, 0.9; and step size increase rate, 1.1. Here, 50% of the observed data were used as training samples (100 samples), and the remaining 50% was used to assess samples. Each sample is a set of data, which contains two input data (FIFFB and SIFFB) and their corresponding feeding decision (continue or stop feeding). And it can be represented by a set: [FIFFB SIFFB DECISION]. The FIFFB and SIFFB were calculated from the captured images and represented the flocking index and struggle strength of the feeding behavior, respectively, in the ANFIS model. The feeding decision was obtained by human observation. When the fish did not respond to food, or eat only pellets that fall directly in front of them and do not move toward food, a value of 0 was scored. Otherwise, fish move freely between food items and consume all food that is presented or fish move to take food but return to their original positions, a value of 1 was scored (Øverli et al., 2006).

To increase the probability of making a correct feeding decision, the membership function was important for training the ANFIS. In this study, the bell-shape MF was chosen to train the ANFIS model. Three fuzzy subsets scatter (big), moderate (middle) and flocking (small) were selected to cover the discourse [380, 620] of the first input linguistic variable FIFFB. Their membership functions and distributions are presented in Fig. 9a. Three fuzzy subsets, almost no snatching (weak), moderate snatching (medium) and violent snatching (strong), were selected to cover the discourse [0, 0.35] of the SIFFB. Their membership functions and distributions are presented in Fig. 10a. The results of the MF of two linguistic input variables after training are presented in Figs. 9 and 10b. Compared with the MF before training in Figs. 9 and 10a, the MF changes in the FIFFB and SIFFB were obvious after training. The trained linguistic labels “middle” and “medium” became narrower, indicating that the probability of the uncertainty of a feeding decision was reduced and the probability of a deterministic feeding decision was increased. These results were attributed to the fact that ANFIS can strengthen the ability to address the uncertainty and imprecision of the system (Amiryousefi et al., 2011). Therefore, the rules based on the linguistic labels on the two sides of “middle” and “medium” are increasingly important in the feeding decision-making. The benefit is that the output of the ANFIS model was more sensitive than before training. Based on the original image, it was found that the fish did not respond to feed and scattered when the linguistic labels were “weak” and “big”. Fish moved to take food in “middle” and “medium” cases. Fish violently snatched and consumed all the feed provided in “strong” and “big” cases. These findings were also consistent with the criteria for classifying feeding intensity by Øverli et al. (2006). Finally, the FLC model achieved the final MFs of the adaptive parameters for the primary linguistic values in the ANFIS model.

Fig. 11 presents the input–output ANFIS surface for the training results of the two input linguistic variables of the FIFFB and SIFFB. This

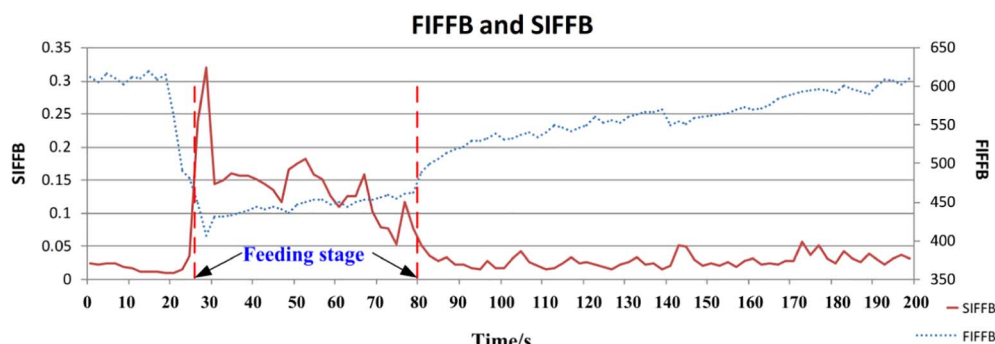


Fig. 7. Curve variation trends of the FIFFB and SIFFB.

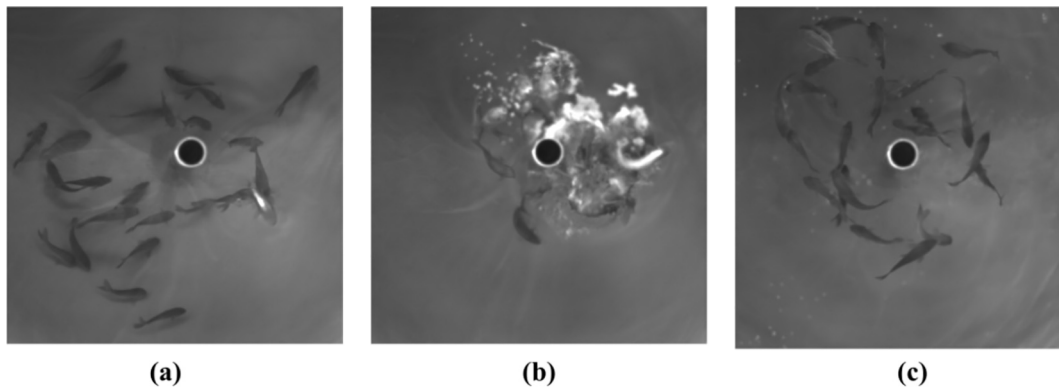


Fig. 8. Examples images of individual stages. (a) Before feeding; (b) feeding stage; (c) after feeding.

surface was created during the training phase. This surface was non-linear and monotonic and illustrates how the ANFIS model will respond to varying values of the FIFFB and SISSB. From this surface, it is clear that the output increases with reductions in the FIFFB and increases in SISSB and vice versa. After training by the hybrid method, 9 “if-then” fuzzy rules were obtained to complete the fuzzification process (Fig. 12).

To verify the performance of the model and improve the accuracy of feeding decisions, the output of the ANFIS model was compared with the appetite quantitative results obtained by human observation. The feeding decision of the ANFIS model can be achieved by defining the threshold using the training data results. Fig. 13a used the training data (100 sets) as input to test the performance between the output of the ANFIS and the true value. If the training data (marked as “o”) and the

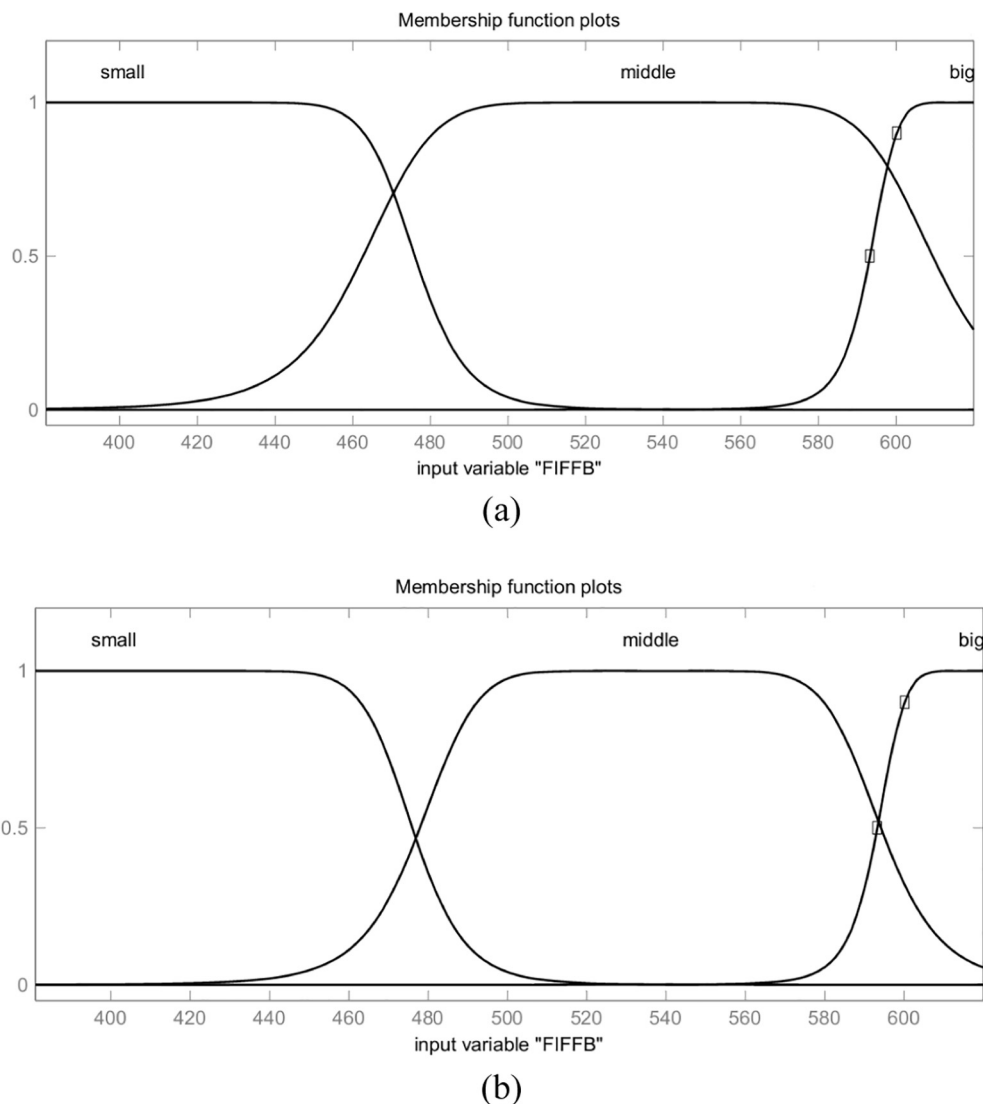


Fig. 9. Membership functions of the FIFFB: (a) before training and (b) after training.

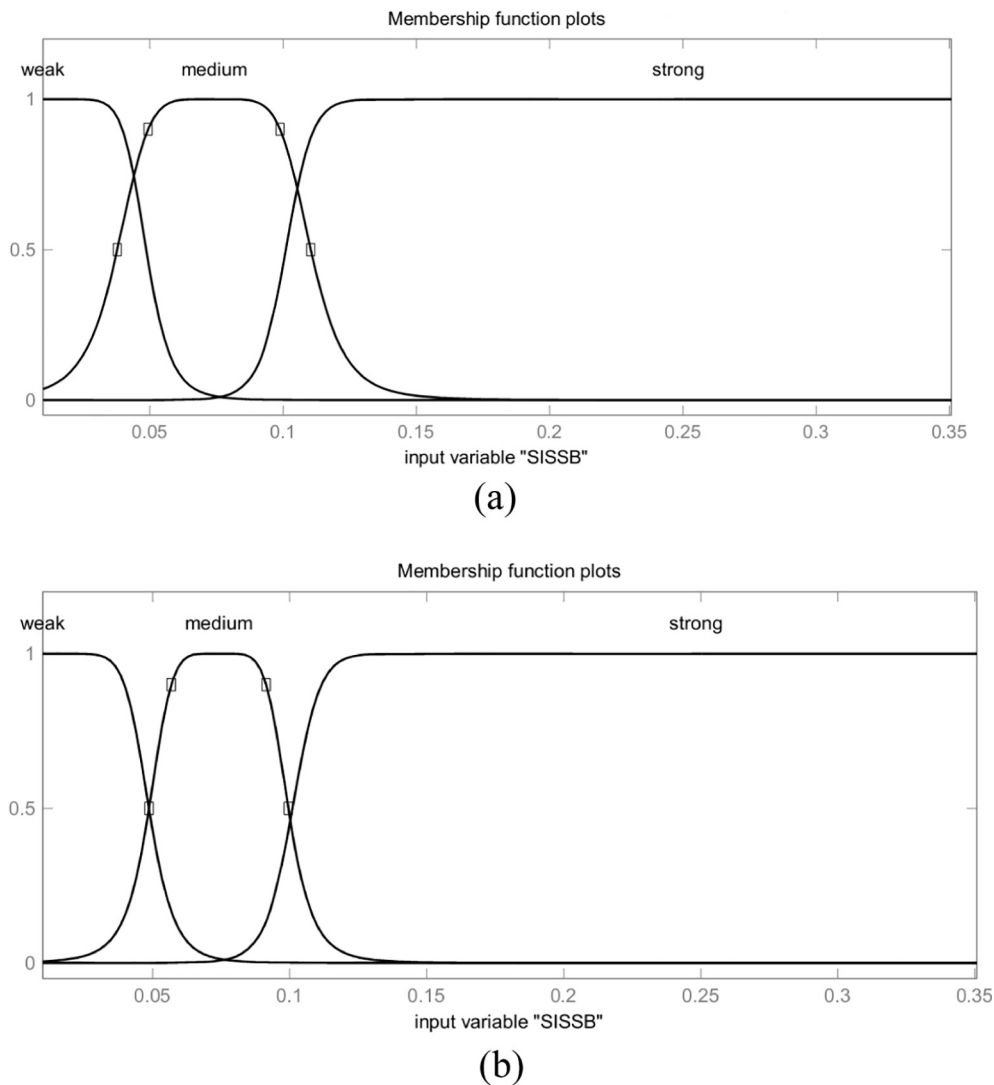


Fig. 10. Membership functions of the SIFFB: (a) before training and (b) after training.

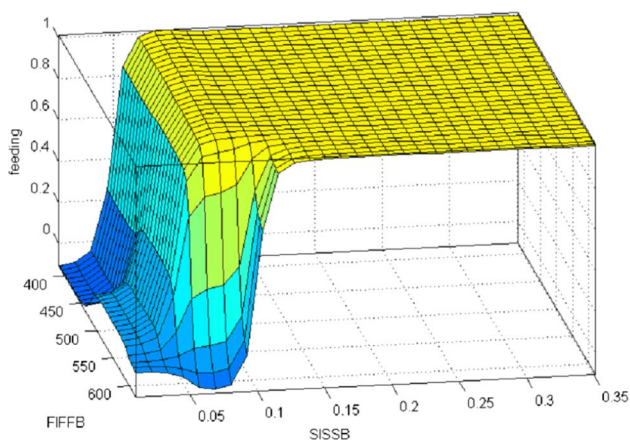


Fig. 11. Three-dimensional surface map.

actual output of ANFIS (marked as “*”) are on the same side of the threshold, the feeding decision was correctly judged. If not, an incorrect decision was made. As shown in Fig. 13a, when the threshold was set as 0.55, the accuracy of decision-making for the ANFIS model was the highest at 98%. Therefore, if the output of the ANFIS was less than 0.55, indicating that the fish has no appetite, feeding should be stopped at

this time. Otherwise, feeding should continue. The results indicate that the output of training data was close to the expected data, and the RMSE of the training data results was 0.17. Fig. 13b presents the ANFIS decision result of the checking data. The accuracy was 97%, and the RMSE was 0.16, indicating that the ANFIS's decision-making output was generally similar to the results of human observation.

However, errors in the feeding decision were noted. In Fig. 13a and b, the arrow indicates a sample with an incorrect decision. Upon analyzing the images of the samples with incorrect decisions, the first type of wrong decision occurs when the “continue feeding” were judged as “stop feeding”. This phenomenon can be explained that the difference in social hierarchies (Benhaïm et al., 2017), response time of fish to feed (Løkkeborg et al., 2014) and swimming ability (Lee et al., 2003) cause asynchrony in the FIFFB and SIFFB, which leads to the erroneous decisions. Another type of wrong decision occurs when the “stop feeding” were judged as “continue feeding”. This finding is attributed to the fact that after feeding, individual fish swam to the surface to catch the bait, resulting in changes in behavior indicators. New algorithms should be developed to solve the issue in a subsequent study. In particular, suspicious data could be removed or new data could be provided by interpolation or fitting (Sarrafz, 2003).

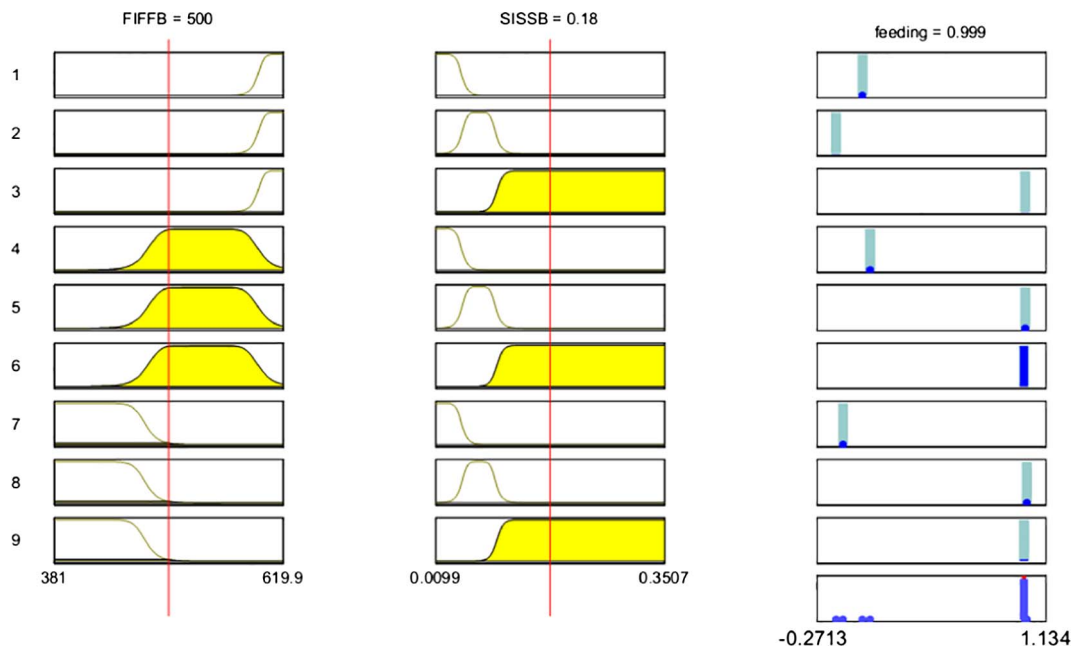


Fig. 12. Nine if-then rules.

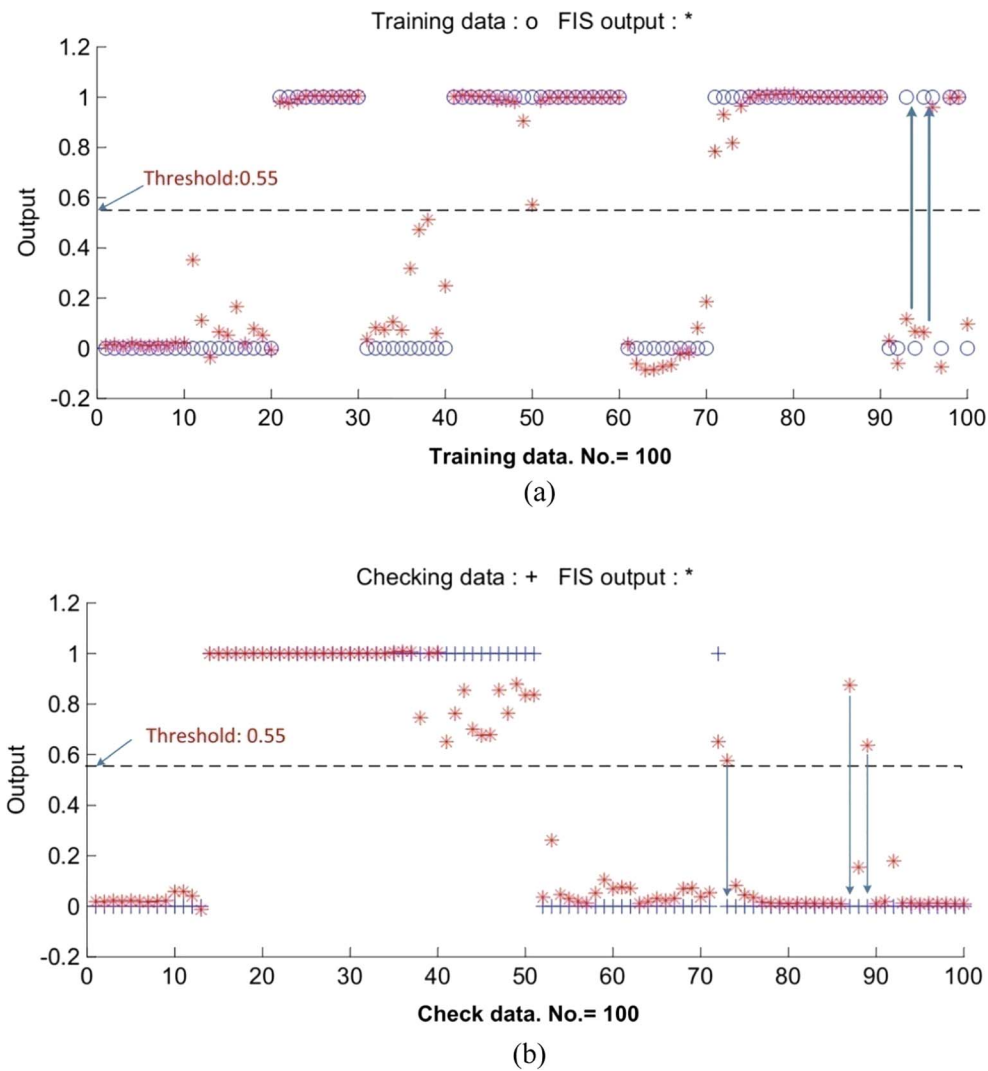


Fig. 13. ANFIS decision result: (a) training error: 0.17; and (b) check error: 0.16. The arrow indicates a sample with incorrect decisions.

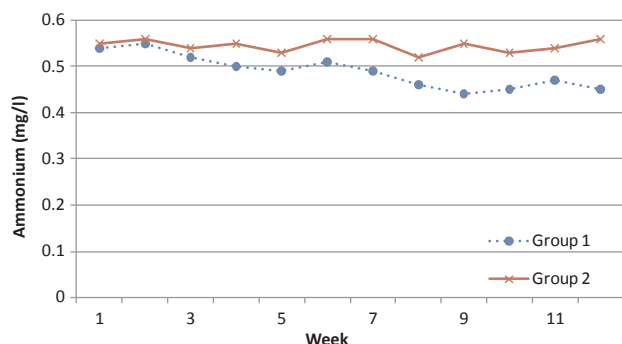


Fig. 14. Ammonia nitrogen concentration curves in two groups.

3.3. Performance of the method

The experiment lasted from June 2017 to August 2017. Two groups of experiments were performed simultaneously. Group 1 was fed in accordance with the proposed method, whereas group 2 was fed with a feeding rate of 2%. With regard to the daily feeding times, both groups were fed twice a day (8:00 and 16:00).

3.3.1. Water quality parameter

Ammonia is the main product of fish protein catabolism and participates in bait decomposition. Studies have demonstrated that 60% of the feed in aquaculture systems was in the form of tiny particles. The decomposition of these particles consumes oxygen and produces ammonia and other toxic substances that affect fish welfare and cause a heavy burden on filtration and oxygenation equipment (Chang et al., 2005). High concentrations of suspended solids can also reduce water transparency and influence the image quality. This parameter can be measured by turbidity.

In extensive aquaculture systems, the water quality parameters were monitored at different frequencies. According to the study of Carbajal-Hernández et al. (2012), the measurements of pH and ammonium should be taken at least one time weekly. In this study, pH and ammonium measurements were obtained at 7:30 before the fish were fed for the first time.

The changes in ammonia nitrogen in two groups are presented in Fig. 14. The overall ammonia concentration in group 2 was consistently increased compared with that in group 1 because the environment and other factors that affect the appetite of fish were considered. Then, the feeding amount in group 1 was adjusted, thus reducing the feed waste and resulting in a relatively low ammonia nitrogen concentration. However, group 2 was fed according to the feeding table, resulting in more feed loss when the fish appetite was not strong. The un-removed feed increased the ammonium concentration. Turbidity also exhibited a similar performance. The maximum turbidity values in groups 1 and 2 were 2.7 mg/l and 5.1 mg/l, respectively. These values were caused by a large amount of unused dissolved solid feed particles in group 2 and reduced feed waste in group 1. In addition, compared with the

beginning of the experiment, the ammonia nitrogen concentration in group 1 gradually decreased and finally stabilized at approximately 0.45 mg/l. In group 2, the concentration of ammonia fluctuated between 0.5 and 0.6 mg/l. The reason is that prior to the experiment, the fish need to be maintained in the experimental system to adapt to the environment and avoid stress. However, because of the normal feeding operation, the system accumulated a certain concentration of ammonia nitrogen and was basically stable. After the experiment started, the system removed a portion of the accumulated ammonia nitrogen as a result of reduced feed waste in group 1. Therefore, the changing trend of ammonia nitrogen concentration in group 1 was gradually reduced and finally stabilized, whereas the concentration of ammonia nitrogen in group 2 was generally unaltered. Obviously, the reduction in ammonia concentration reduces the pressure on the aquaculture system, providing better fish welfare.

In the two experimental groups, the pH values were maintained between 7.7 and 8.5, and the dissolved oxygen concentration was maintained between 5.8 and 8.2 mg/l. These values are acceptable for the normal growth of tilapia.

3.3.2. Fish growth performance

The growth and feed consumption of fish in experiments are important factors in evaluating the method performance. Table 1 presents the average weight of the fish at the beginning and end in each tank and the WGR, SGR, and FCR in each group. No significant differences were noted in the growth status between both groups. The differences in WGR and SGR between the two groups was not significant ($P > .05$). However, the FCR value was 1.74 ± 0.06 for group 1 and 1.95 ± 0.06 for group 2, which decreased by approximately 10.77%, and the difference was significant ($P < .05$). Thus, this system effectively reduces feed cost. This is because in the modern intensive aquaculture system, the feed supply is relatively abundant. Producers can provide almost 100% of the nutritional requirements to meet the normal growth of fish (Soto-Zarazúa et al., 2010). Therefore, the growth status of the two groups did not differ but the conversion efficiency of feed in group 1 was significantly better. The results were acceptable and revealed that the ANFIS-based intelligent feeding control method could greatly reduce the waste of feed and improve the economic benefit under the premise of ensuring the normal growth of fish, thereby reducing water pollution and promoting fish welfare.

In addition, this method was validated in tilapia, a typical swimming fish, via feeding experiments. However, the effects of the method remain unknown for other species of swimming fish. For example, the recognition effect is typically better for a scaly fish compared with a fish without scales in image processing (Zhou et al., 2017b). In addition, the feeding habits of some species (Houlihan et al., 2007) may cause some differences in the method results. Therefore, this method must be validated on more fish species to enhance its applicability in a commercial fish farm.

Table 1
Performance evaluation index.

Group	Tank No	Initial weight(g)	Final weight(g)	WGR%	SGR%	FCR%
1	1	219.54 ± 62.35	583.21 ± 6.25	165.65	1.16	1.74
	2	220.11 ± 61.09	601.01 ± 5.68	173.05	1.20	1.69
	3	229.41 ± 47.19	595.35 ± 23.06	159.51	1.14	1.80
	Average	223.02 ± 5.5	593.19 ± 9.1	166.07 ± 6.78 ^a	1.17 ± 0.03 ^a	1.74 ± 0.06 ^a
2	4	224.28 ± 60.99	589.32 ± 13.26	162.76	1.15	2.01
	5	217.37 ± 62.17	598.59 ± 35.89	175.28	1.21	1.89
	6	223.96 ± 66.77	603.29 ± 6.19	169.37	1.18	1.95
	Average	221.87 ± 3.9	597.07 ± 7.1	169.13 ± 6.23 ^a	1.18 ± 0.03 ^a	1.95 ± 0.06 ^b

Note: Different letters with the same column denote significant ($p < .05$).

4. Conclusions

In this paper, an intelligent feeding decision method for fish was proposed. Using near infrared machine vision and an ANFIS model, automatic feeding control was realized according to the appetites of fish. The results indicate that the ANFIS model can achieve a feeding decision accuracy of 98%. Compared with the feeding table method, no significant difference in growth was noted ($P > .05$). However, the FCR can be reduced by 10.77%, and water pollution can be reduced. Further applications of the method in production can significantly improve economic efficiency and provide a theoretical foundation for the development of new intelligent feeding equipment or systems. However, this method requires additional validation in other fish species before it is used in commercial-scale fish farms.

Acknowledgements

The work was supported by the National Key Research and Development Program of China (2017YFD0701705) and the Beijing Natural Science Foundation (4184089).

References

- Amiryousefi, M.R., Mohebbi, M., Khodaiyan, F., Asadi, S., 2011. An empowered adaptive neuro-fuzzy inference system using self-organizing map clustering to predict mass transfer kinetics in deep-fat frying of ostrich meat plates. *Comput. Electron. Agric.* 76, 89–95.
- Benhaim, D., Akian, D.D., Ramos, M., Ferrari, S., Yao, K., Bégout, M.-L., 2017. Self-feeding behaviour and personality traits in tilapia: a comparative study between *Oreochromis niloticus* and *Sarotherodon melanocheilus*. *Appl. Anim. Behav. Sci.* 187, 85–92.
- Carbajal-Hernández, J.J., Sánchez-Fernández, L.P., Carrasco-Ochoa, J.A., Martínez-Trinidad, J.F., 2012. Immediate water quality assessment in shrimp culture using fuzzy inference systems. *Expert Syst. Appl.* 39, 10571–10582.
- Chang, C.M., Fang, W., Jao, R.C., Shyu, C.Z., Liao, I.C., 2005. Development of an intelligent feeding controller for indoor intensive culturing of eel. *Aquacult. Eng.* 32, 343–353.
- Downey, A.B., Koutsopoulos, H.N., 1993. Primitive-based classification of pavement cracking images. *J. Transp. Eng.* 119, 402–418.
- Duarte, S., Reig, L., Oca, J., 2009. Measurement of sole activity by digital image analysis. *Aquacult. Eng.* 41, 22–27.
- Farokhi, S., Flusser, J., Ullah Sheikh, U., 2016. Near infrared face recognition: a literature survey. *Comput. Sci. Rev.* 21, 1–17.
- Houlihan, D., Boujard, T., Jobling, M., 2007. *Food Intake in Fish*. Blackwell Science Ltd, New York, USA.
- Hu, J., Li, D., Duan, Q., Han, Y., Chen, G., Si, X., 2012. Fish species classification by color, texture and multi-class support vector machine using computer vision. *Comput. Electron. Agric.* 88, 133–140.
- Hung, C.-C., Tsao, S.-C., Huang, K.-H., Jang, J.-P., Chang, H.-K., Dobbs, F.C., 2016. A highly sensitive underwater video system for use in turbid aquaculture ponds. *Sci. Rep.* 6, 31810.
- Iglesias Nuno, A., Arcay, B., Cotos, J.M., Varela, J., 2005. Optimisation of fishing predictions by means of artificial neural networks, Anfis, functional networks and remote sensing images. *Expert Syst. Appl.* 29, 356–363.
- Jang, J.S.R., 1993. ANFIS: adaptive-network-based fuzzy inference systems. *IEEE Trans. Syst. Man Cybernet.* 23, 665–685.
- Johansson, D., Ruohonen, K., Kiessling, A., Oppedal, F., Stiansen, J.-E., Kelly, M., Juell, J.-E., 2006. Effect of environmental factors on swimming depth preferences of Atlantic salmon (*Salmo salar* L.) and temporal and spatial variations in oxygen levels in sea cages at a fjord site. *Aquaculture* 254, 594–605.
- Juell, J.E., Furevik, D.M., Bjørndal, Å., 1993. Demand feeding in salmon farming by hydroacoustic food detection. *Aquacult. Eng.* 12, 155–167.
- Løkkeborg, S., Siikavuopio, S.I., Humborstad, O.-B., Utne-Palm, A.C., Ferter, K., 2014. Towards more efficient longline fisheries: fish feeding behaviour, bait characteristics and development of alternative baits. *Rev. Fish Biol. Fish.* 24, 985–1003.
- Lall, S.P., Tibbetts, S.M., 2009. Nutrition, feeding, and behavior of fish. *Vet. Clin. North Am. Exot. Anim. Pract.* 12, 361–372.
- Lee, C.G., Devlin, R.H., Farrell, A.P., 2003. Swimming performance, oxygen consumption and excess post-exercise oxygen consumption in adult transgenic and ocean-ranched coho salmon. *J. Fish Biol.* 62, 753–766.
- Li, D., Xu, L., Liu, H., 2017. Detection of uneaten fish food pellets in underwater images for aquaculture. *Aquacult. Eng.* 78, 85–94.
- Lin, K., Zhou, C., Xu, D., Guo, Q., Yang, X., Sun, C., 2018. Three-dimensional location of target fish by monocular infrared imaging sensor based on a L-z correlation model. *Infrared Phys. Technol.* 88, 106–113.
- Liu, Z., Li, X., Fan, L., Lu, H., Liu, L., Liu, Y., 2014. Measuring feeding activity of fish in RAS using computer vision. *Aquacult. Eng.* 60, 20–27.
- Loo, J.L., 2013. The use of vision in a sustainable aquaculture feeding system. *Res. J. Appl. Sci. Eng. Technol.* 6, 3658–3669.
- Mallekh, R., Lagardère, J.P., Eneau, J.P., Cloutour, C., 2003. An acoustic detector of turbid feeding activity. *Aquaculture* 221, 481–489.
- Martins, C.I., Galhardo, L., Noble, C., Damsgård, B., Spedicato, M.T., Zupa, W., Beauchaud, M., Kulczykowska, E., Massabuau, J.C., Carter, T., 2012. Behavioural indicators of welfare in farmed fish. *Fish Physiol. Biochem.* 38, 17.
- Mollazade, K., Omid, M., Akhlaghian Tab, F., Kalaj, Y.R., Mohtasebi, S.S., Zude, M., 2013. Analysis of texture-based features for predicting mechanical properties of horticultural products by laser light backscattering imaging. *Comput. Electron. Agric.* 98, 34–45.
- Moreda, G.P., Muñoz, M.A., Ruiz-Altisent, M., Perdigones, A., 2012. Shape determination of horticultural produce using two-dimensional computer vision – A review. *J. Food Eng.* 108, 245–261.
- Øverli, Ø., Sørensen, C., Nilsson, G.E., 2006. Behavioral indicators of stress-coping style in rainbow trout: Do males and females react differently to novelty? *Physiol. Behav.* 87, 506–512.
- Papandroulakis, N., Markakis, G., Divanach, P., Kentouri, M., 2000. Feeding requirements of sea bream (*Sparus aurata*) larvae under intensive rearing conditions: Development of a fuzzy logic controller for feeding. *Aquacult. Eng.* 21, 285–299.
- Pautsina, A., Císař, P., Štys, D., Terjesen, B.F., Espmark, Å.M.O., 2015. Infrared reflection system for indoor 3D tracking of fish. *Aquacult. Eng.* 69, 7–17.
- Pinkiewicz, T.H., Purser, G.J., Williams, R.N., 2011. A computer vision system to analyse the swimming behaviour of farmed fish in commercial aquaculture facilities: A case study using cage-held Atlantic salmon. *Aquacult. Eng.* 45, 20–27.
- Rola, W.R., Hasan, M.R., 2007. Economics of aquaculture feeding practices: a synthesis of case studies undertaken in six Asian countries.
- Sadoul, B., Evouna Mengues, P., Friggens, N.C., Prunet, P., Colson, V., 2014. A new method for measuring group behaviours of fish shoals from recorded videos taken in near aquaculture conditions. *Aquaculture* 430, 179–187.
- Sarfraz, M., 2003. A rational cubic spline for the visualization of monotonic data: an alternate approach. *Comput. Graph.-UK* 27, 107–121.
- Sefeedpari, P., Rafiee, S., Akram, A., Komleh, S.H.P., 2014. Modeling output energy based on fossil fuels and electricity energy consumption on dairy farms of Iran: Application of adaptive neural-fuzzy inference system technique. *Comput. Electron. Agric.* 109, 80–85.
- Shcherbakov, D., Knörzer, A., Espenhahn, S., Hilbig, R., Haas, U., Blum, M., 2013. Sensitivity differences in fish offer near-infrared vision as an adaptable evolutionary trait. *PLoS ONE* 8, 1446–1446.
- Soto-Zarazúa, G.M., Rico-García, E., Ocampo, R., Guevara-González, R.G., Herrera-Ruiz, G., 2010. Fuzzy-logic-based feeder system for intensive tilapia production (*Oreochromis niloticus*). *Aquacult. Int.* 18, 379–391.
- Sun, M., Hassan, S.G., Li, D., 2016. Models for estimating feed intake in aquaculture: A review. *Comput. Electron. Agric.* 127, 425–438.
- Virgen-Navarro, L., Herrera-López, E.J., Corona-González, R.I., Arriola-Guevara, E., Guatemala-Morales, G.M., 2016. Neuro-fuzzy model based on digital images for the monitoring of coffee bean color during roasting in a spouted bed. *Expert Syst. Appl.* 54, 162–169.
- Wu, T.-H., Huang, Y.-I., Chen, J.-M., 2015. Development of an adaptive neural-based fuzzy inference system for feeding decision-making assessment in silver perch (*Bidyanus bidyanus*) culture. *Aquacult. Eng.* 66, 41–51.
- Xu, J., Liu, Y., Cui, S., Miao, X., 2006. Behavioral responses of tilapia (*Oreochromis niloticus*) to acute fluctuations in dissolved oxygen levels as monitored by computer vision. *Aquacult. Eng.* 35, 207–217.
- Zhangying, Y., Jian, Z., Zhiying, H., Songming, Z., Jianping, L., Huanda, L., Yunjie, R., 2016. Behavioral characteristics and statistics-based imaging techniques in the assessment and optimization of tilapia feeding in a recirculating aquaculture system. *Trans. ASABE* 59, 345–355.
- Zhao, J., Bao, W.J., Zhang, F.D., Ye, Z.Y., Liu, Y., Shen, M.W., Zhu, S.M., 2017. Assessing appetite of the swimming fish based on spontaneous collective behaviors in a recirculating aquaculture system. *Aquacult. Eng.* 78, 196–204.
- Zhao, J., Gu, Z., Shi, M., Lu, H., Li, J., Shen, M., Ye, Z., Zhu, S., 2016. Spatial behavioral characteristics and statistics-based kinetic energy modeling in special behaviors detection of a shoal of fish in a recirculating aquaculture system. *Comput. Electron. Agric.* 127, 271–280.
- Zhou, C., Sun, C., Lin, K., Xu, D., Guo, Q., Chen, L., Yang, X., 2018. Handling water reflections for computer vision in aquaculture. *Trans. ASABE*. <http://dx.doi.org/10.13031/trans.12466>. (in press).
- Zhou, C., Xu, D., Lin, K., Sun, C., Yang, X., 2017a. Intelligent feeding control methods in aquaculture with an emphasis on fish: a review. *Rev. Aquacult.* <http://dx.doi.org/10.1111/raq.12218>. (in press).
- Zhou, C., Yang, X., Zhang, B., Lin, K., Xu, D., Guo, Q., Sun, C., 2017b. An adaptive image enhancement method for a recirculating aquaculture system. *Sci. Rep.* 7, 6243.
- Zhou, C., Zhang, B., Lin, K., Xu, D., Chen, C., Yang, X., Sun, C., 2017c. Near-infrared imaging to quantify the feeding behavior of fish in aquaculture. *Comput. Electron. Agric.* 135, 233–241.
- Zion, B., 2012. The use of computer vision technologies in aquaculture – a review. *Comput. Electron. Agric.* 88, 125–132.